Phase inhomogeneities and lattice expansion near T_c in the $Mg^{11}B_2$ superconductor

2001 J. Phys.: Condens. Matter 13 L795

(http://iopscience.iop.org/0953-8984/13/35/101)

INSTITUTE OF PHYSICS PUBLISHING JOURNAL OF PHYSICS: CONDENSED MATTER

J. Phys.: Condens. Matter **13** (2001) L795–L802 PII: S0953-8984(01)26471-6

LETTER TO THE EDITOR

Phase inhomogeneities and lattice expansion near T_c in the $Mg^{11}B_2$ superconductor

S Margadonna[1], T Muranaka[2], K Prassides[3,4], I Maurin[3], K Brigatti[3], R M Ibberson[5], M Arai[6], M Takata[7] and J Akimitsu[2]

[1] Department of Chemistry, University of Cambridge, Cambridge CB2 1EW, UK
[2] Department of Physics, Aoyama-Gakuin University, Chitosedai, Setagaya-ku, Tokyo 157-8572, Japan
[3] School of Chemistry, Physics and Environmental Science, University of Sussex, Brighton BN1 9QJ, UK
[4] Institute of Materials Science, NCSR 'Demokritos', 15310 Ag. Paraskevi, Athens, Greece
[5] The ISIS Facility, Rutherford Appleton Laboratory, Didcot, Oxon OX11 0QX, UK
[6] KEK, Institute of Materials Structure Science, Tsukuba, Ibaraki 305-0801, Japan
[7] Department of Applied Physics, Nagoya University, Nagoya 464-8603, Japan

Received 3 July 2001
Published 16 August 2001
Online at stacks.iop.org/JPhysCM/13/L795

Abstract

High-resolution powder neutron diffraction has been used to study the crystal structure of the $Mg^{11}B_2$ superconductor ($T_c = 39.2$ K) prepared at high pressure in the temperature range 2 to 293 K. The experimental data provide clear evidence of temperature-independent phase inhomogeneity, which was modelled by coexisting $Mg_{1+\delta}B_2$ phases. Precise structural information for temperatures near T_c also reveals extremely small volume and c-axis discontinuities, consistent with the existence of a specific heat anomaly at T_c.

1. Introduction

The discovery of superconductivity in MgB_2 at $T_c = 39$ K [1] has attracted much interest because of the simplicity in chemical composition, crystal structure and electronic properties of this system. Detailed information on the properties of MgB_2, especially related to the nature of superconductivity, has already been accumulated by means of a variety of structural and electronic probes. MgB_2 adopts a hexagonal structure (AlB_2-type, space group $P6/mmm$) [2] which is analogous to that of intercalated graphite with all hexagonal prismatic sites of the primitive graphitic structure (found in hexagonal BN) completely filled and resulting in two interleaved B and Mg layers. In addition, as a result of essentially complete charge transfer from Mg to the boron 2D sheets, the latter are isoelectronic with graphite. Despite the simplicity of its structure, MgB_2 displays an intricate interplay of interactions between electrons and phonons. The superconducting transition temperature is almost at the extreme end of the range of values of T_c predicted by the BCS theory for conventional superconductors.

The experimental investigations suggest that it is a BCS-type superconductor with confirmed isotope and other related effects [3, 4].

Studies of doping at the Mg site or the 2D B sheets have been carried out to reveal the effect of the electron concentration on T_c [5–8]. Several reports of the gradual suppression of superconductivity with increasing doping level, x, have been presented for the series $Mg_{1-x}Al_xB_2$ [5], $MgB_{2-x}C_x$ [6], $Mg_{1-x}Li_xB_2$ [7] and $Mg_{1-x}Mn_xB_2$ [8]. In addition, T_c has been found to decrease with applied pressure in MgB_2, consistent with the mediation of the pairing interaction by phonons [9–11].

More recently, however, evidence has started to accumulate that effects associated with Mg non-stoichiometry and phase inhomogeneity are present in different MgB_2 samples [12]. For instance, the pressure dependence of the electrical resistivity and the superconducting transition temperature in MgB_2 are strongly sample dependent [13]. TEM imaging has revealed that the structural features of MgB_2 depend systematically on the synthesis conditions, especially applied pressure, which may influence the presence of stacking faults and planar defects [14]. In addition, the assertion that MgB_2 could be microscopically non-stoichiometric is supported by the work of Xue *et al*, suggesting that most of the samples which were synthesized in a 1:2 Mg/B ratio are actually non-stoichiometric by up to 5–10% [15]. These effects could imply the coexistence in the same sample of phases with differing Mg/B ratios, although x-ray and neutron diffraction studies have not as yet shown any evidence of such a multiphase behaviour [11, 16].

In an attempt to investigate the structural properties of MgB_2 in detail, high-resolution powder neutron diffraction measurements were performed at 2 and 293 K. The diffraction profiles showed the presence of temperature-independent peak splittings and/or strong asymmetries, which were modelled in terms of coexisting MgB_2 phases with varying Mg/B ratios. The evolution of the structure as a function of temperature near T_c was also investigated, revealing a weak slope discontinuity of the volume expansivity at T_c, with its principal component associated with the interlayer c-axis.

2. Experimental procedure

As natural-abundance B has a very large neutron absorption cross-section, the MgB_2 sample used in this work was prepared by reaction of Mg powder (99.9%) and crystalline isotopically enriched ^{11}B (99.52%, Eagle Picher). The reactants were wrapped in Ta foil, placed in a C crucible and heated at 900 °C for five hours and at 850 °C for six hours under argon pressures of 196 and 175 MPa, respectively; this was followed by quenching to room temperature. $Mg^{11}B_2$ was superconducting with $T_c = 39.2$ K. Phase purity was examined by means of powder x-ray diffraction, revealing a high-quality sample with small impurities content of MgO at <4%, MgB_4 at <1% and C at <1% levels.

Temperature-dependent structural work was undertaken with the high-resolution neutron powder diffractometer, HRPD, at ISIS, Rutherford Appleton Laboratory, UK. 8.85 g of the material were placed in a rectangular vanadium sample holder and positioned in a liquid helium cryostat, accessing the temperature range 2 to 300 K. The 1 m high-flux sample position (resolution: $\Delta d/d = 8 \times 10^{-4}$) was used in these measurements, with backscattering, 90° and low-angle detector banks being monitored simultaneously. The phasing of the HRPD choppers was such that the time-of-flight window between 20 and 120 ms, equivalent to a d-spacing range of 0.4 to 2.4 Å, could be observed. High-statistics data sets, binned in $\Delta t/t = 10^{-4}$ steps, were collected at 2 and 293 K, reaching total currents of 82 and 106 μA, respectively. Shorter runs (total current 8.6 μA per run) were also recorded between 4 and 53 K in steps of 1 K. The data were analysed with the Rietveld method using the GSAS software [17].

3. Results

Detailed inspection of the high-statistics neutron powder diffraction profile collected at 293 K in the d-spacing range 0.6–2.3 Å shows, as expected, that essentially all the Bragg reflections could be indexed with an AlB_2-type hexagonal structure (space group $P6/mmm$) in agreement with previous reports [2]. The AlB_2-type structure contains graphite-like boron layers, which are separated by hexagonal close-packed layers of metal. Each metal lies directly above and below the centre of hexagonal boron rings. The neutron powder diffraction profile was then refined by the Rietveld method using as the starting model the reported structure where the B and Mg atoms are placed at the 1a (0, 0, 0) and 2d (1/3, 2/3, 1/2) sites, respectively. From analysing the fitted pattern, it was clear that even though all the positions of the Bragg reflections were well accounted for, particular problems were encountered in their peak shape. The high-resolution neutron powder diffractometer HRPD has a well-defined instrumental line shape, which is described in terms of a modified Ikeda–Carpenter function. In order to describe anisotropic broadening effects, the peak shape is defined by a function resulting from the convolution of two back-to-back exponentials with a pseudo-Voigt function. This modified Ikeda–Carpenter function is incorporated in the GSAS software [17] and was employed in the course of the refinement. Despite the use of the appropriate peak-shape function, it was not possible to account for the asymmetry present in all the Bragg reflections in a physically meaningful way. The asymmetry is particularly evident in the (002) reflection ($d \approx 1.76$ Å) which shows a well-defined shoulder on the high-d-spacing side ($\Delta d/d \approx 2 \times 10^{-3}$), implying the possibility of multiphase behaviour (inset in figure 1) and the presence of minority phase(s) with somewhat larger lattice parameter(s) c.

In order to explore the possibility of the coexistence of more than one phase, a series of Rietveld refinements of different structural models were performed on the diffraction profile collected at 293 K. At first, a single-phase MgB_2 model was used and the profile coefficients were carefully refined in an attempt to model the peak asymmetry. The final result was unsatisfactory ($\chi^2 = 3.61$) and, due to the poor fitting of the peak shape, the calculated positions of the Bragg reflections were shifted from the experimental ones resulting in a biased set of lattice constants. From studying the pronounced asymmetry of the (002) reflections and the much less pronounced asymmetry of the (200) reflections ($d \approx 1.76$ and 1.41 Å, respectively), it was clear that both comprised several peaks, which were partially resolved.

A second series of refinements was then undertaken based on a two-phase model in which two MgB_2 phases were used differing only in lattice dimensions. Resolution of the coexisting phases is possible because of the high resolution of HRPD. On using this model the refinement improved significantly ($\chi^2 = 2.99$) and the peak-shape description was considerably more satisfactory (figure 1), resulting in a reliable set of lattice constants $a_1 = 3.084\,78(3)$ Å and $c_1 = 3.519\,56(4)$ Å for phase 1 (fraction = 63%) and $a_2 = 3.085\,59(6)$ Å and $c_2 = 3.528\,17(10)$ Å for phase 2 (fraction = 37%). Within this model, we also attempted to establish the differences in composition between the two phases present. Such differences could arise for a number of reasons, including non-stoichiometry of the Mg and/or B sites as well as disorder between them. The neutron scattering lengths of Mg and ^{11}B are 5.375 and 6.65 fm, respectively. The lack of significant contrast between these makes determination of the exact stoichiometries and any degree of site disorder difficult. We note however that the difference in interlayer cell dimension of the two phases (0.24%) is substantially larger than the intralayer one (0.03%), suggesting that phase 2 is richer in Mg than phase 1. We thus assumed the B layers to be filled, and independently refined the site occupancies of Mg. The resulting stoichiometries were $Mg_{0.992(4)}B_2$ and $Mg_{1.066(9)}B_2$ for phases 1 and 2, respectively. The presence of strong statistical correlations makes the results of also refining the B stoichiometry

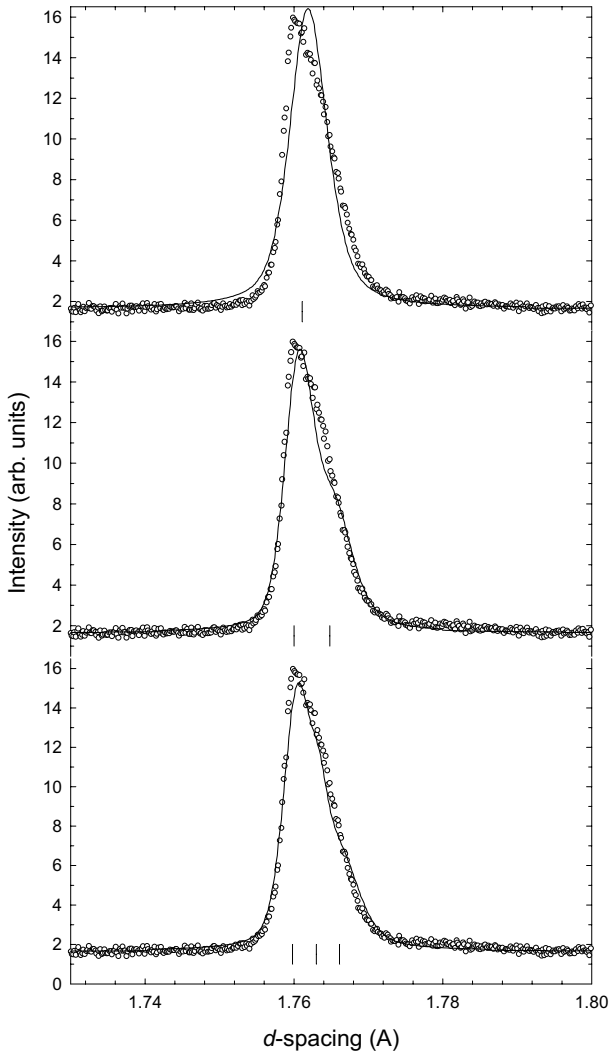

Figure 1. Observed (points) and calculated (solid line) neutron powder diffraction profiles for $Mg^{11}B_2$ at 293 K in the range 1.73–1.80 Å corresponding to the (002) reflection for the three structural models explored in this work: single phase (top), two-phase (middle) and three-phase (bottom panel) refinement.

less reliable. Nonetheless, even then there is broad agreement that, while phase 1 is essentially stoichiometric, phase 2 is characterized by an excess of Mg and, to a lesser extent, of B. In the final stages of the refinement, the anisotropic temperature factors of Mg and B were also refined. The final results are summarized in table 1.

Further improvement in the refinement and in the observed reflection peak-shape description (figure 1) was achieved by using a three-phase model in which the three phases differ only in cell parameters. The refinement again proceeded smoothly and the final results are summarized in table 2. With this three-phase model, it was possible to account even better for the strong peak asymmetry and, as is shown in figure 2 ($\chi^2 = 2.83$, $R_{exp} = 5.5\%$), the neutron diffraction profile is well described. However, due to the complexity of the model

Table 1. Refined structural parameters for $Mg_{1+\delta}{}^{11}B_2$ at 293 and 2 K based on the two-phase Rietveld refinements described in the text.

	$Mg_{1+\delta}{}^{11}B_2$, 293 K		$Mg_{1+\delta}{}^{11}B_2$, 2 K	
	Phase 1	Phase 2	Phase 1	Phase 2
a (Å)	3.08478(3)	3.08559(6)	3.08152(2)	3.08459(5)
c (Å)	3.51956(4)	3.52817(10)	3.51325(5)	3.52379(12)
Fraction (%)	62.9(2)	37.1(3)	64.5(2)	35.5(3)
δ	−0.008(4)	0.066(9)	−0.010(5)	0.054(9)
U_{11}(Mg) (Å^2)	0.00613(34)		0.00330(65)	
U_{33}(Mg) (Å^2)	0.00780(54)		0.00250(74)	
U_{12}(Mg) (Å^2)	0.00306(17)		0.00115(33)	
U_{11}(B) (Å^2)	0.00277(23)		0.00318(45)	
U_{33}(B) (Å^2)	0.00652(32)		0.00402(57)	
U_{12}(B) (Å^2)	0.00138(12)		0.00199(22)	

Table 2. Refined structural parameters for $Mg^{11}B_2$ at 293 and 2 K based on the three-phase Rietveld refinements described in the text.

	$Mg^{11}B_2$, 2 K		
	Phase 1	Phase 2	Phase 3
a (Å)	3.08113(3)	3.08399(6)	3.08611(18)
c (Å)	3.51263(5)	3.52141(15)	3.52871(30)
Fraction (%)	63.9(5)	20.8(5)	15.9(5)
	$Mg^{11}B_2$ 293 K		
	Phase 1	Phase 2	Phase 3
a (Å)	3.08395(3)	3.08563(7)	3.08815(8)
c (Å)	3.51967(5)	3.52597(17)	3.53240(15)
Fraction (%)	65.1(7)	18.4(4)	16.5(4)

and the increase in the number of refinable parameters, it did not prove possible to refine independently the fractional occupancies and anisotropic thermal factors of the Mg and B atoms for the three phases.

High-statistics neutron diffraction data of the $Mg^{11}B_2$ sample were also collected at 2 K. In agreement with earlier reports, inspection of the diffraction profile shows that no phase transition is observed in this temperature range with the Bragg reflections still displaying the same pronounced asymmetry as was already discussed for the room temperature data. Series of Rietveld refinements were then attempted following the same procedure. The one-phase ($\chi^2 = 3.29$), two-phase ($\chi^2 = 2.84$) and three-phase models were all tested and the final results are summarized in tables 1 and 2. Once again, the peak asymmetry was described increasingly well with an increasing number of coexisting phases with the three-phase model giving the best agreement factors ($\chi^2 = 2.67$, $R_{exp} = 6.30\%$).

TOF neutron powder diffraction measurements were also performed on the same sample of $Mg^{11}B_2$ on heating from 4 to 53 K in steps of 1 K. For the Rietveld analysis only the data collected on the backscattering bank of detectors were used and every data set was rebinned in steps of $\Delta t/t = 3 \times 10^{-4}$. Due to the high correlation among the parameters in the

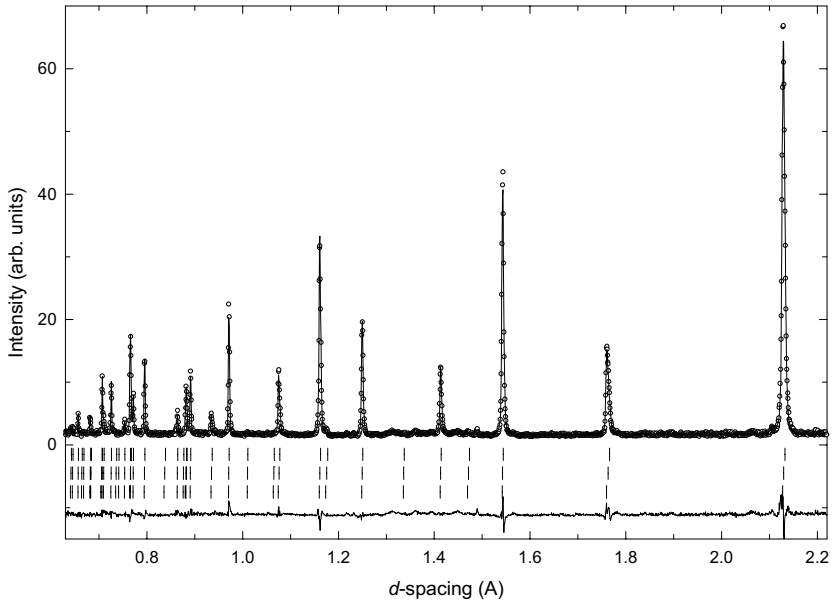

Figure 2. Observed (points) and calculated (solid line) neutron powder diffraction profiles for $Mg^{11}B_2$ at 293 K in the range 0.63–2.22 Å. The lower solid line shows the difference profile and the three sets of ticks mark the positions of the Bragg reflections of the three coexisting phases.

three-phase model and the lower statistics of these measurements, the two-phase model was chosen to perform the Rietveld analysis at each temperature. For every data set only the Gaussian contribution to the peak-width function and the lattice constants were refined, while the phase fractions were fixed to those obtained by the analysis of the high-statistics runs. In addition, the ratios between the values of the cell parameters of the two phases (a_1/a_2 and c_1/c_2) were constrained to those obtained in the 2 K refinement. The Rietveld analysis proceeded smoothly up to 53 K (hexagonal lattice constants at 53 K: $a_1 = 3.081\,54(3)$ Å, $c_1 = 3.513\,39(8)$ Å, $a_2 = 3.084\,62(3)$ Å, $c_2 = 3.513\,39(8)$ Å; agreement factors: $\chi^2 = 1.60$, $R_{exp} = 11.62$). The extracted temperature evolution of the lattice constants of the major phase 1 is shown in figure 3.

4. Discussion

The high-resolution neutron powder diffraction measurements employed in this work to study the crystal structure of a MgB_2 sample prepared at high pressure have revealed the presence of significant inhomogeneities which were modelled employing a phenomenological multiphase structural model, comprising coexisting $Mg_{1+\delta}B_2$ compositions/intergrowths with $\delta \geqslant 0$. The quality of the Rietveld refinements improves as we move from a two- to a three-phase structural model, implying the possibility of the presence of a distribution of phase compositions which peaks at $\delta = 0$. The presence of excess Mg in the boron interlayer spacing leads to an evident increase in the lattice constant c. This is accompanied by a smaller expansion of the boron basal-plane dimension a, which may reflect the competition of steric and electronic effects. The present structural data shed some light on the differing physical properties shown by MgB_2 samples prepared by different synthesis routes. However, despite the obvious inhomogeneities present in the sample, the observed superconducting transition onset is very sharp.

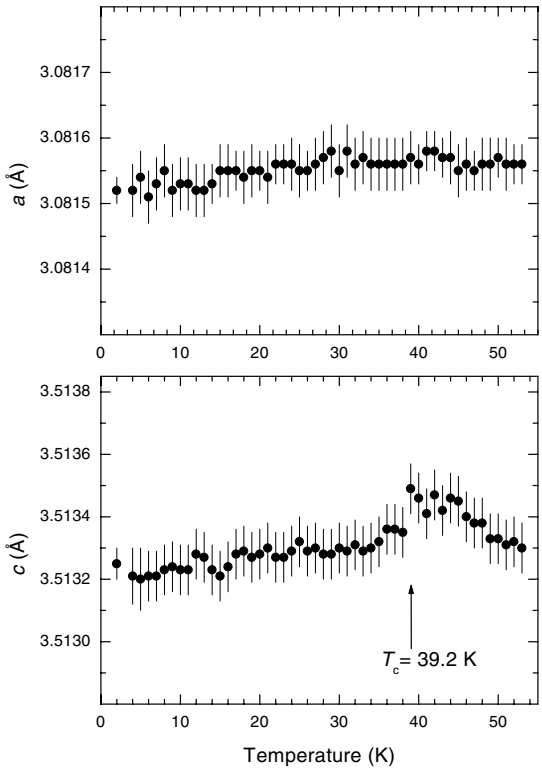

Figure 3. Temperature evolution of the hexagonal lattice constants a and c of $Mg^{11}B_2$ in the range 2–53 K.

The temperature evolution of the hexagonal lattice constants in the temperature range 2 to 53 K is shown in figure 3. In this temperature range, the expansivities are extremely small ($\alpha_a = 9 \times 10^{-7}$ Å K^{-1}, $\alpha_c = 4 \times 10^{-6}$ Å K^{-1}), though somewhat more pronounced for the interlayer axis c, consistent with the bonding anisotropy between intralayer and interlayer directions. Time-of-flight powder neutron diffraction is particularly good for determining the lattice parameters and their temperature evolution to a very high degree of both precision and accuracy because there is effectively no zero-point correction due to the fixed detector geometry. Thus very importantly, while the variation in the a-axis direction is found to be completely smooth, there is some evidence for a discontinuity in the magnitude of the c-axis parameter at T_c. A small increase of $\Delta c = (14 \pm 16) \times 10^{-5}$ Å at 39 K is clearly seen, despite the large estimated standard deviations, because the expansivity is extremely small in this temperature range. This is followed by a gradual decrease as the temperature increases further.

The slope discontinuity in the expansivity of the c-axis parameter is also reflected in the temperature dependence of the unit-cell volume V, leading to a volume expansivity anomaly at T_c of $\partial(\Delta V)/\partial T = (34 \pm 72) \times 10^{-6}$ $Å^3$ K^{-1}. This is reminiscent of the situation encountered in other superconducting systems in which slope discontinuities have also been identified in the volume expansivity at T_c [18, 19]. These are invariably small (for instance, in $YBa_2Cu_3O_7$, $\partial(\Delta V)/\partial T = (11 \pm 16) \times 10^{-5}$ $Å^3$ K^{-1} [20]) and can be related to the specific heat anomaly at T_c and the variation of the transition temperature with pressure through the relationship $\partial(\Delta V)/\partial T = (\mathrm{d}T_c/\mathrm{d}P)(\Delta C/T_c)$. In recent specific heat measurements, $\Delta C/T_c$ for $Mg^{11}B_2$ was obtained as 3.44 mJ K^{-2} mol^{-1} [21], while values of the pressure coefficient, $\mathrm{d}T_c/\mathrm{d}P$,

in the range 0.11–0.20 K kbar^{-1} have been reported in the literature [9–11]. These yield a value for the expected volume expansivity anomaly, $\partial(\Delta V)/\partial T$, for MgB_2 in the range (6–11) $\times 10^{-6}$ Å^3 K^{-1}, of the same order of magnitude as that extracted above.

5. Conclusions

In conclusion, high-resolution neutron powder diffraction has been used to study in detail the structural properties of $Mg^{11}B_2$ prepared by the hot isostatic pressure technique. While the majority of the sample is essentially stoichiometric with a formula unit close to $Mg_{1.0}B_2$, evidence has been presented of inhomogeneities in the Mg and, to a lesser extent, in the B distribution, leading to the presence of $Mg_{1+\delta}B_2$ phases/intergrowths with $\delta > 0$. Detailed temperature-dependent diffraction measurements in the vicinity of T_c have also revealed evidence for a small anomaly in the volume expansivity with a principal component along c and which could be associated with the second-order superconducting phase transition.

We thank the Rutherford Appleton Laboratory for the provision of neutron beamtime. SM thanks Jesus College, Cambridge, for a Research Fellowship. The work at Aoyama-Gakuin University was partially supported by a Grant-in-Aid for Science Research from the Ministry of Education, Science, Sports and Culture, Japan and by a grant from CREST.

References

[1] Nagamatsu J, Nakagawa N, Muranaka T, Zenitani Y and Akimitsu J 2001 *Nature* **410** 63
[2] Jones M E and Marsh R E 1954 *J. Am. Chem. Soc.* **76** 1434
[3] Bud'ko S L, Lapertot G, Petrovic C, Cunningham C E, Anderson N and Canfield P C 2001 *Phys. Rev. Lett.* **86** 1877
Hinks D G, Claus M and Jorgensen J D 2001 *Nature* **411** 357
[4] Schmidt H, Zasadzinski J F, Gray K E and Hinks D G 2001 *Preprint* cond-mat/0102389
Karapetrov G, Iavarone M, Kwok W K, Crabtree G W and Hinks D G 2001 *Phys. Rev. Lett.* **86** 4374
[5] Slusky J S, Rogado N, Regan K A, Hayward M A, Khalifah P, He T, Inumaru K, Loureiro S M, Haas M K, Zandbergen H and Cava R J 2001 *Nature* **410** 342
[6] Takenobu T, Ito T, Chi D H, Prassides K and Iwasa Y 2001 *Preprint* cond-mat/0103214
Takenobu T, Ito T, Chi D H, Prassides K and Iwasa Y 2001 *Phys. Rev.* B submitted
[7] Zao Y G, Zhang X P, Qiao P T, Zhang H T, Jia S L, Cao B S, Zhu M H, Han Z H, Wang X L and Gu B L 2001 *Preprint* cond-mat/0103007
[8] Xu S, Moritomo Y, Kato K and Nakamura A 2001 *Preprint* cond-mat/0104534
Xu S, Moritomo Y, Kato K and Nakamura A 2001 *J. Phys. Soc. Japan* submitted
[9] Lorenz B, Meng R L and Chu C W 2001 *Phys. Rev.* B **64** 012507
[10] Saito E, Takenobu T, Ito T, Iwasa Y, Prassides K and Arima T 2001 *J. Phys.: Condens. Matter* **13** L267
[11] Jorgensen J D, Hinks D G and Short S 2001 *Phys. Rev.* B **63** 224522
[12] Zhao Y G, Zhang X P, Qiao P T, Zhang H T, Jia S L, Cao B S, Zhu M H, Han Z H, Wang X L and Gu B L 2001 *Preprint* cond-mat/0105053
[13] Monteverde M, Nunez-Regueiro M, Rogado N, Regan K A, Hayward M A, He T, Loureiro S L and Cava R J 2001 *Science* **292** 75
[14] Li J Q, Li L, Zhou Y Q, Ren Z A, Che G C and Zhao Z X 2001 *Preprint* cond-mat/0104350
[15] Xue Y Y, Meng R L, Lorenz B, Meen J K, Sun Y Y and Chu C W 2001 *Preprint* cond-mat/0105478
[16] Nishibori E, Takata M, Sakata M, Tanaka H, Muranaka T and Akimitsu J 2001 *J. Phys. Soc. Japan* at press
[17] Larsen A C and Von Dreele R B *GSAS Software, Los Alamos National Laboratory Report* LAUR 86-748
[18] Millis A J and Rabe K M 1988 *Phys. Rev.* B **38** 8908
[19] You H, Welp U and Fang Y 1991 *Phys. Rev.* B **43** 3660
[20] David W I F, Edwards P P, Harrison M R, Jones R and Wilson C C 1988 *Nature* **331** 245
[21] Bouquet F, Fisher R A, Phillips N E, Hinks D G and Jorgensen J D 2001 *Preprint* cond-mat/0104206